

Numerical simulation of inelastic frictional spheres in simple shear flow

By C. K. K. LUN AND A. A. BENT

Department of Engineering, Dalhousie University, Halifax, Nova Scotia, Canada B3H 3J5

(Received 1 September 1992 and in revised form 18 June 1993)

A numerical program is developed to simulate an assembly of inelastic frictional spheres inside a control volume undergoing rapid shearing motion induced by the top and bottom moving periodic boundaries. A sticking–sliding collision model is used to emulate binary collisions of real particles. After the flow has reached a steady state, ensemble averages of macroscopic properties such as translational and rotational granular temperatures, and kinetic and collisional stresses at different solids concentrations are obtained. The present results are compared with previous theoretical, numerical and experimental works, and favourable agreement is found among them. The simulation results show that the stresses are anisotropic and decrease with decreasing coefficient of restitution and increasing friction coefficient. At high solids fraction, above about 0.5, there exists a critical concentration where the layering effects of particles, the formation of high-density microstructures and the increase in correlation of particle velocities are the major causes of abrupt changes in flow properties.

1. Introduction

In the past decade or so, a number of experimental investigations, theoretical analyses and computer simulations have contributed towards the fundamental understanding of governing mechanisms for rapid granular flows. Although each approach has its own advantages and limitations, together they help to enrich our knowledge of the subject, which is of crucial importance in a wide variety of industrial, geophysical and scientific applications. The subject has recently been reviewed by a number of researchers such as Savage (1989, 1993), Campbell (1986, 1990), Jenkins (1987) and Richman (1986).

One of the limitations of laboratory experiments is that it is rather difficult to develop instrumentation that is capable of measuring flow properties such as velocity, density and granular temperature profiles inside the granular material without disturbing the flow field. Nonetheless, valuable information on stresses at relatively high solids concentrations and shear rates has been obtained from annular shear cell experiments (Savage & Sayed 1984; Hanes & Inman 1985; Craig, Buckholz & Domoto 1986, 1987).

Following the approaches of molecular dynamics and Monte Carlo methods, computer simulations of rapid granular flows have become excellent tools to provide detail information about the basic flow mechanics, which otherwise might be difficult to obtain in physical experiments. The present study focuses on the simulation of idealized inelastic frictional spheres in simple shear flow. We follow the deterministic approach of molecular dynamics in which the particle positions and velocities are

known at all times. Ensemble averages of macroscopic properties are obtained after the flow has reached a steady state. The results are compared with previous theoretical, numerical and experimental works.

2. Collision model

Consider a collision between two inelastic frictional spherical particles 1 and 2 each of diameter σ and having translational velocities \mathbf{c}_1 and \mathbf{c}_2 , angular velocities $\boldsymbol{\omega}_1$ and $\boldsymbol{\omega}_2$, respectively. The total relative velocity, \mathbf{g}_{12} , at contact point just prior to the collision is

$$\mathbf{g}_{12} = \mathbf{c}_{12} - \frac{1}{2}\sigma\mathbf{k} \times \boldsymbol{\Omega}, \quad (2.1)$$

where $\mathbf{c}_{12} = \mathbf{c}_1 - \mathbf{c}_2$ and $\boldsymbol{\Omega} = \boldsymbol{\omega}_1 + \boldsymbol{\omega}_2$. According to the collision model proposed by Lun & Savage (1987) and Lun (1991), the components of \mathbf{g}_{12} are changed in a collision such that

$$\mathbf{k} \cdot \mathbf{g}'_{12} = -e(\mathbf{k} \cdot \mathbf{g}_{12}), \quad \mathbf{k} \times \mathbf{g}'_{12} = -\beta(\mathbf{k} \times \mathbf{g}_{12}), \quad (2.2a, b)$$

where \mathbf{k} is the unit vector along the centreline from particle 1 to particle 2, primed quantities denote post-collisional values, e is the usual coefficient of restitution in the normal direction, and β may be called the coefficient of restitution in the tangential direction at the *point of contact*. For brevity, e and β will be called the normal and tangential coefficients of restitution respectively.

Using (2.2a, b) in (2.1) the relationships between the pre- and post-collisional velocities can be written as

$$m(\mathbf{c}_1 - \mathbf{c}'_1) = m(\mathbf{c}'_2 - \mathbf{c}_2) = \mathbf{J}, \quad (2.3)$$

$$I(\boldsymbol{\omega}'_1 - \boldsymbol{\omega}_1) = I(\boldsymbol{\omega}'_2 - \boldsymbol{\omega}_2) = -\frac{1}{2}\sigma(\mathbf{k} \times \mathbf{J}), \quad (2.4)$$

and

$$\mathbf{J} = m\eta_2\mathbf{g}_{12} + m(\eta_1 - \eta_2)\mathbf{k}(\mathbf{k} \cdot \mathbf{g}_{12}), \quad (2.5)$$

where m is the mass of a particle, \mathbf{J} is the impulse, $\eta_1 = \frac{1}{2}(1 + e)$, $\eta_2 = \frac{1}{2}(1 + \beta)K/(1 + K)$, and $K = 4I/(m\sigma^2)$ is a non-dimensional moment-of-inertia parameter. For a uniform solid sphere $K = \frac{2}{5}$, and for a solid disk $K = \frac{1}{2}$.

From physical considerations, experimental evidence and theoretical analysis of friction surface deformations (Goldsmith 1960; Maw, Baber & Fawcett 1976, 1981), it is apparent that the normal coefficient of restitution, e , depends on the inelasticity and impact velocity in the normal direction whereas the tangential coefficient of restitution, β , depends on the tangential inelasticity, particle surface friction and impact velocity. In general, e decreases with increasing normal impact velocity. According to Maw *et al.*, there can be no slip, micro slip or complete slip in the contact zone of the colliding spheres (see also Johnson 1982). As a result, β can be either positive or negative.

In general, the coefficients e , and β can have values in the ranges $0 \leq e \leq 1$ and $-1 \leq \beta \leq 1$. The value of $\beta = -1$ represents perfectly smooth particles, whereas $\beta = 1$ corresponds to perfectly elastic, perfectly rough ones. Campbell (1989) used $\beta = 0$, which depicted particles with infinite friction, in his numerical simulation model. Depending upon the impact velocities and the material properties, the tangential coefficient of restitution can change significantly. The actual collision process is rather complex, for it involves elastic-plastic deformation in the vicinity of the contact zone and wave propagation inside the material. For simplicity, an idealized sticking-sliding collision model is employed in the present study in which instantaneous binary collisions are assumed.

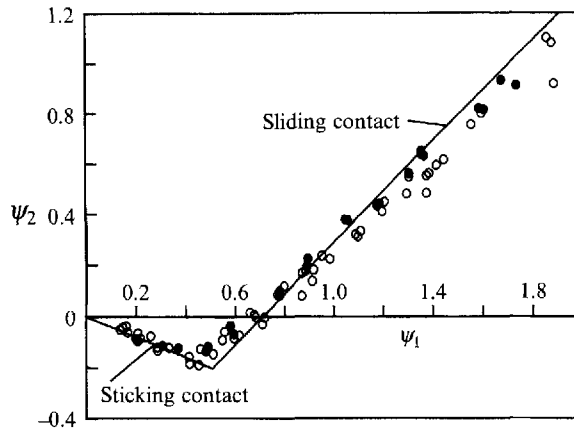


FIGURE 1. Variations of non-dimensional tangential rebound velocity, ψ_2 , with tangential incident velocity, ψ_1 . Comparison of predictions from equations (2.11) for sticking contact and (2.12) for sliding contact (solid lines) with experimental measurements of Maw (1976) using steel pucks of diameters: \circ , 3 in; \bullet , 4 in.

In oblique impacts, the normal and tangential impulses at the contact point are assumed to obey the Coulomb law of friction. In the case of the tangential impulse being less than the product of the friction coefficient and the normal impulse, i.e. $|\mathbf{k} \times \mathbf{J}| < \mu |\mathbf{k} \cdot \mathbf{J}|$, sticking or no-slip contact occurs. From (2.2a, b), the post-collisional normal relative velocity, V'_n , and the surface tangential relative velocity, V'_s , are simply given by

$$V'_n = -eV_n, \quad V'_s = -\beta_0 V_s, \tag{2.6a, b}$$

where β_0 is regarded as a phenomenological constant characterizing the restitution of velocity in the tangential direction for sticking contacts, and in general, $0 \leq \beta_0 \leq 1$. Positive β_0 denotes particles rebounding with reverse spin caused by the restoration of elastic energy in the tangential direction. Both e and β_0 are considered to be constant coefficients which have been averaged over particle impact velocity and are appropriate for a particular range of granular temperatures.

On the other hand, when the tangential impulse is greater than or equal to the product of the friction coefficient and the normal impulse, sliding contact occurs and the following equality applies:

$$|\mathbf{k} \times \mathbf{J}| = \mu |\mathbf{k} \cdot \mathbf{J}|. \tag{2.7}$$

From (2.5) and (2.7), the tangential coefficient of restitution is found explicitly as

$$\beta = -1 + \mu(1+e)(1+1/K) V_n/V_s; \tag{2.8}$$

thus from (2.2b) we have

$$V'_s = -\beta V_s. \tag{2.9}$$

In their kinetic theories for rough inelastic spheres, Lun & Savage (1987) and Lun (1991) regarded the tangential coefficient of restitution, β , as merely a constant averaged over the entire range of sticking and sliding contracts. Nakagawa (1988) used a collision model similar to the present one in his kinetic theory for disks in which the rebound tangential relative velocity for all sticking contact was assumed to be zero, i.e. $\beta_0 = 0$. Walton (1988) employed essentially the same collision model as the present one

in his numerical simulations in which the effect of particle surface friction on stresses was studied by fixing β_0 and varying μ from zero to unity.

Maw (1976) and Maw *et al.* (1981) performed experiments to measure the rotational and translational velocities of steel pucks before and after impact with fixed blocks of similar material. The steel pucks were symmetrically sliced by spark erosion from commercial ball bearings. A friction coefficient of 0.123 was measured for the steel pucks by using an inclined plane. The range of coefficient of restitution obtained in the experiments was $0.87 \leq e \leq 0.99$ and the mean value was 0.93.

The experimental results may be presented in terms of non-dimensional pre- and post-collisional tangential velocities, defined as

$$\psi_1 = V_s/V_n, \quad \psi_2 = -V'_s/V'_n. \quad (2.10 a, b)$$

By using (2.2 *a, b*) and (2.8)–(2.10 *a, b*), the sticking contact solution gives

$$\psi_2 = -\beta_0 \psi_1 \quad (2.11)$$

while the sliding contact solution yields

$$\psi_2 = \psi_1 - \mu(1+e)(1+1/K). \quad (2.12)$$

In figure 1, predictions from (2.11) and (2.12) are compared with the measurements of Maw (1976). The value of β_0 for steel is found to be about 0.4 by averaging the slopes of the data points in the sticking contact region. The mean value of $e = 0.93$ is used in the computations. In general, there is reasonable agreement between the predictions and the test data. Perhaps one weakness of the present model is that the transition from sticking to sliding occurs rather abruptly as compared to the real case. Nonetheless, the model is simple and yields reasonable results.

3. Simple shear flow

A numerical model is developed to simulate shear flow of hard spheres with mean velocity of $\mathbf{u} = u(y)\mathbf{e}_x$. Shearing of bulk material inside a control volume is achieved by means of periodic image cells moving with velocities $+U\mathbf{e}_x$ on the top and $-U\mathbf{e}_x$ on the bottom of the control volume. When a particle leaves the bottom, it re-enters the control volume with an increase in velocity of $U\mathbf{e}_x$ through the top at a position determined by its image in the upper image cell. A similar reassignment of velocity and position is applied to particles that leave the top and re-enter the bottom. Each side of the control volume is bounded by a periodic stationary image cell. Such an arrangement for the control volume and its images has become a standard model to imitate the case of simple shear flow (see, for example, Lees & Edwards 1972; Walton & Braun 1986 *a, b*; Allen & Tildesley 1987; Campbell 1989).

In shearing flows, energy and momentum are transferred by means of interparticle collisions and the kinetic motion of an individual particle. The rate of work done on the bulk solids by the moving boundaries in simple shear flow is balanced by the collisional rate of energy dissipation through particle inelasticity and surface friction. As a result, the flow can reach a steady state in which the dynamic properties such as rotational and translational granular temperatures have unique values.

Particles are initially arranged in an array of face-centred-cubic (FCC) lattices inside a control volume. Such an arrangement can provide a maximum solids fraction of 0.74. Solids fraction is defined as the ratio of the volume occupied by the solids to the total volume. Because the assumption of instantaneous binary collisions can break down at

high concentrations, the maximum solids fraction that can be sheared in the present model is found to be about 0.65 for particles with $e = 0.95$. Depending on whether the solids fraction is less or greater than 0.35, the present computer code generates a control volume having 81 particles in an initial $3 \times 9 \times 3$ FCC array or 144 particles in a $4 \times 8 \times 4$ FCC array (referring to the number of particles in the x -, y -, and z -directions respectively). The main reason for using two different total numbers of particles is to reduce computation time.

Each particle is initiated with an instantaneous translational velocity composed of a random component C and a mean component according to a linear velocity profile, i.e. $\mathbf{u} = (U/H)y\mathbf{e}_x$, where H is the height of the control volume. The magnitude of the fluctuating velocity is initially equated to the 'thermal' speed of the bulk solids, i.e. $C = (3T_{ti})^{1/2}$; T_{ti} is the initial mean translational granular temperature and can be set arbitrarily. The three directions of the fluctuation velocity for each particle are randomly assigned. In the present study, high T_{ti} is used for all simulations unless specified otherwise.

Once T_{ti} is chosen, the simulation may begin. The computer program selects consecutively one particle at a time from a particle list and searches for potential colliding partners from the rest. Only particles that are located within the nearest neighbourhood of the chosen particle are considered for possible interactions. The program then determines the time δt for each possible binary collision by using an elementary kinematic equation of motion. Each pair of potential colliding partners and its δt value are recorded in chronological order on a collisional list and a time list respectively. The length of the collisional and time lists can vary depending on the solids concentration in the system; for moderate solids fraction, the typical list length is about 100. After each particle in the particle list has been selected, the flow time is incremented by the time taken for the first collision and all particle velocities and positions are updated. The transfer of linear and angular momentum in each collision is recorded for statistical averaging. The collided pair and their potential colliding partners are registered in a check list after they are removed from the collisional list. Each particle in the check list is selected for the search of colliding partners and each potential colliding pair is inserted into the collisional list according to its time for collision. After the check list is exhausted, the flow time is incremented again. The process is repeated until a prescribed number of collisions per particle for ending the simulation is reached. Depending on the initial condition, convergence to a steady state normally occurs at about 500 collisions per particle. After steady state is reached, ensemble averages for flow properties are taken at intervals of 200, 500 or sometimes 2000 collisions per particle. No significant difference in the result is found by varying the size of the ensemble provided that it is statistically sufficiently large. Each simulation run is performed up to a minimum of 3000, and in some cases 4000, collisions per particle.

The control volume is partitioned into i strips with equal dimensions. On the basis of the statistical integrals of transport properties provided by the kinetic theories (e.g. Lun 1991), one can deduce an equivalent set of discrete non-dimensional formulae for determining the distribution of properties such as mean velocity, granular temperature and stresses in the system. Let $\bar{V}_i = V_i/\sigma^3$ be the non-dimensional volume of the i th strip and N_i be the total number of particles in it. The non-dimensional quantities such as solids fraction ν , mean velocity $\bar{\mathbf{u}} = \mathbf{u}/U$, mean particle spin $\bar{\omega}_0 = \omega_0/(U/\sigma)$, translational temperature $\bar{T}_t = T_t/U^2$, rotational temperatures $\bar{T}_r = T_r/U^2$, kinetic stresses $\bar{\mathbf{P}}_k = \mathbf{P}_k/[\rho_p(\sigma U/H)^2]$, collisional stresses $\bar{\mathbf{P}}_c = \mathbf{P}_c/[\rho_p(\sigma U/H)^2]$, kinetic angular

momentum fluxes $\bar{\mathbf{L}}_k = \mathbf{L}_k / [\rho_p \sigma^3 (U/H)^2]$ and collisional angular momentum fluxes $\bar{\mathbf{L}}_c = \mathbf{L}_c / [\rho_p \sigma^3 (U/H)^2]$ may be expressed as

$$\nu_i = \pi N_i / 6 \bar{V}_i, \quad (3.1)$$

$$\bar{\mathbf{u}}_i = \frac{1}{N_i} \sum_j \bar{\mathbf{c}}_j, \quad (3.2)$$

$$\bar{\boldsymbol{\omega}}_{0i} = \frac{1}{N_i} \sum_j \bar{\boldsymbol{\omega}}_j, \quad (3.3)$$

$$\bar{T}_{ti} = \frac{1}{3N_i} \sum_j \bar{\mathbf{C}}_j \cdot \bar{\mathbf{C}}_j, \quad (3.4)$$

$$\bar{T}_{ri} = \frac{K}{12N_i} \sum_j \bar{\mathbf{W}}_j \cdot \bar{\mathbf{W}}_j, \quad (3.5)$$

$$\bar{\mathbf{P}}_{ki} = \frac{\pi \bar{H}^2}{6 \bar{V}_i} \sum_j \bar{\mathbf{C}}_j \bar{\mathbf{C}}_j, \quad (3.6)$$

$$\bar{\mathbf{P}}_{ci} = \frac{\pi \bar{H}^2}{6 \bar{V}_i \bar{\delta} t} \sum_j \bar{\mathbf{J}}_j \mathbf{k}, \quad (3.7)$$

$$\bar{\mathbf{L}}_{ki} = \frac{\pi K \bar{H}^2}{24 \bar{V}_i} \sum_j \bar{\mathbf{C}}_j \bar{\mathbf{W}}_j, \quad (3.8)$$

$$\bar{\mathbf{L}}_{ci} = \frac{\pi \bar{H}^2}{12 \bar{V}_i \bar{\delta} t} \sum_j \mathbf{k} (\mathbf{k} \times \bar{\mathbf{J}}_j), \quad (3.9)$$

where ρ_p is the particle mass density, the index i denotes the i th strip, \sum_j represents the sum over all particles within the strip and $\bar{\mathbf{J}}$ is the non-dimensional impulse transmitted during a binary collision. The non-dimensional fluctuating linear velocity, fluctuating angular velocity, impulse and incremental time are defined as $\bar{\mathbf{C}} = \mathbf{C}/U$, $\bar{\mathbf{W}} = (\boldsymbol{\omega} - \boldsymbol{\omega}_0)/U$, $\bar{\mathbf{J}} = \mathbf{J}/(mU)$ and $\bar{\delta} t = \delta t U/\sigma$ respectively. The total stresses are $\bar{\mathbf{P}} = \bar{\mathbf{P}}_k + \bar{\mathbf{P}}_c$, while the total angular momentum fluxes are $\bar{\mathbf{L}} = \bar{\mathbf{L}}_k + \bar{\mathbf{L}}_c$.

Note that the mean velocity in (3.2), mean particle spin in (3.3), and translational and rotational granular temperature in (3.4) and (3.5) involve arithmetic means whereas the solids fraction in (3.1), kinetic stresses in (3.6), and kinetic angular momentum fluxes in (3.8) require volume averaging. The collisional stresses in (3.7) and collisional angular momentum flux in (3.9) need both volume and time averaging. To be consistent with the kinetic theory, the properties of an individual flow particle are assigned to the strip where the particle centre is found. The position of the impulse action in a collision is designated at the contact point of the colliding pair of flow particles in evaluating the collisional stresses in (3.7) and collisional angular momentum flux in (3.9). In other words, the change of momentum during a binary collision is attributed to the strip where the contact point occurs. Since all positions within the control volume in the simple shear simulations are equally probable in terms of accessibility by the particle centres and the contact points of the particle collisions, the volumes \bar{V}_i used for averaging the solids fraction, kinetic and collisional stresses, and kinetic and collisional angular momentum fluxes are simply equal to the constant volume of the strip itself.

The computer program constantly checks for particle overlaps by determining the distance between each pair of particle centres, which must be no less one particle diameter σ . A tolerance of $1.0 \times 10^{-15} \sigma$ is set in the computation to accommodate possible roundoff error in the numerical functions for the double-precision real numbers used. Furthermore, the transport properties and flow time are monitored periodically in each computation run. If particle overlaps did occur, the flow time would probably advance extremely slowly even after thousands of collisions per particle. All the results presented herein are free of 'particle overlaps'.

Typically, the simulation program running in a 286-PC with a Microway Number Smasher-860-40 MHz coprocessor board takes about 2 to 3 hours of real time to finish 3000 collisions per particle for systems with 81 to 144 particles.

4. Comparisons with previous works

In this section, we study the effects of normal and tangential coefficients of restitution, friction coefficient, solids fraction, dimensions of the control volume and initial translational granular temperature on flow properties such as stresses, temperatures and mean particle spin. The present results are compared with those obtained in the numerical simulations of Walton & Braun (1986*a*) and Campbell (1989), the experimental measurements of Craig *et al.* (1986), and the theoretical predictions of Lun (1991).

Figures 2 and 3 show the variations of non-dimensional stresses (namely three normal stresses, \bar{P}_{xx} , \bar{P}_{yy} , \bar{P}_{zz} , and one shear stress, $|\bar{P}_{xy}|$) with solids fraction, ν , for cases of perfectly smooth spheres (i.e. $\beta = -1$) with $e = 0.95$, 0.8 and 0.6. Substantial agreement is found between the present results, those of Walton & Braun (1986*a*) and the predictions of Lun (1991). The theoretical results obtained by Lun are identical with those of Lun *et al.* (1984) and Jenkins & Richman (1985) for the case of perfectly smooth spheres.

The radial distribution function at contact given by Carnahan & Starling (1969), i.e. $g_0 = (2 - \nu)/[2(1 - \nu)^3]$, is used in the computations of Lun instead of the one originally proposed by Lun & Savage (1987), i.e. $g'_0 = (1 - \nu/\nu_m)^{-2.5\nu_m}$; where ν_m represents the maximum possible solids fraction of the system. The g_0 of Carnahan & Starling was formulated based upon molecular dynamics studies of virial expansions under *equilibrium* conditions and with the use of periodic boundaries. Its predictions are consistent with numerical results for solids fraction up to about 0.55.

On the other hand, Lun & Savage (1986) propose the ad hoc equation for g'_0 which contains the parameters ν_m to account for the finite-size effect of real granular systems which arises partly from the finite geometric constraints imposed by the solid boundaries on the flow particles and partly from the finite size of the particles themselves. Depending on the relative sizes of the particles and the shear zone inside the annulus of the shear cells, the value of ν_m can be as low as about 0.55. As the solids fraction of the system approached ν_m , the stresses increased rapidly with small increment of solids fraction (e.g. Hanes & Inman 1985; Craig *et al.* 1986; Savage & Sayed 1984). By using equation for g'_0 , the theoretical predictions do exhibit to some degree the kind of behaviour of stresses observed in the experiments as ν approaches ν_m . However, we should keep in mind that the kinetic theory of Lun (1991) has not incorporated phenomena such as multiple particle contacts, microstructures and particle layering effects which can strongly influence the stresses at high solids concentrations. In a recent numerical simulation, Savage (1992) used a Couette cell bounded by four periodic stationary sidewalls, along with top and bottom bumpy walls. He found quite

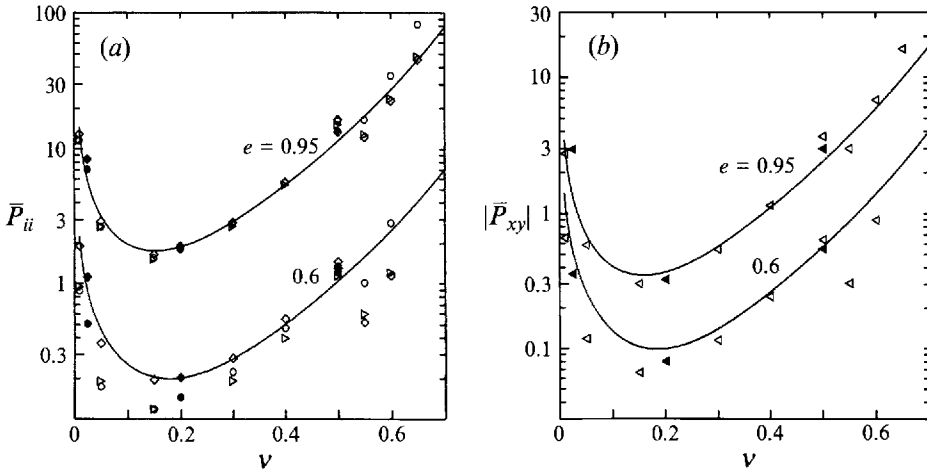


FIGURE 2. Non-dimensional (a) normal stresses and (b) shear stress versus solids fraction ν for simple shear flow. Comparison of present results for perfectly smooth spheres having $e = 0.95$ and 0.6 (\diamond , \bar{P}_{xx} ; \circ , \bar{P}_{yy} ; \triangleright , \bar{P}_{zz} ; \triangleleft , $|\bar{P}_{xy}|$) with predictions of Lun (1991) (solid curves) and results of Walton & Braun (1986) (\blacklozenge , \bar{P}_{xx} ; \bullet , \bar{P}_{yy} ; \blacktriangleleft , $|\bar{P}_{xy}|$).

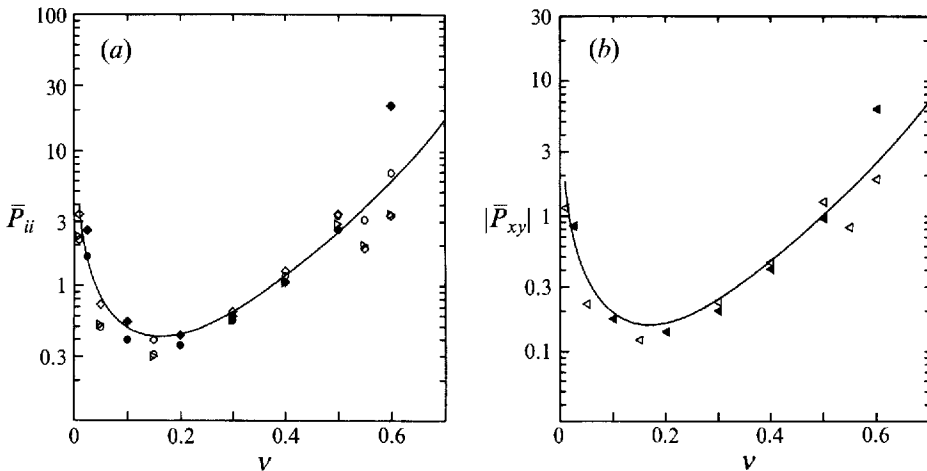


FIGURE 3. As figure 2, but for $e = 0.8$.

the opposite behaviour of stresses at high solids fractions with shear gap height $H = 4\sigma$: the stresses actually decreased with increasing ν . This shows that the rapid increase of stresses at high solids fractions is perhaps not unique, as one might have thought. In the present study, since we are using periodic boundaries on all sides, the control volume may be viewed as a small region within an infinite medium under simple shearing motion. The kind of finite-size effect imposed by the solids boundaries on the flow field is absent. Therefore, it seems more appropriate to use g_0 rather than g'_0 for comparisons between the predictions of the kinetic theory and the present simulation results.

In general the normal stresses are anisotropic (figures 2 and 3); the anisotropy in stresses increases with decreasing e . Since the theory of Lun (1991) assumes isotropic granular temperature distributions, it predicts isotropic stresses. Nevertheless, the predictions compare reasonably well with the majority of the simulation results.

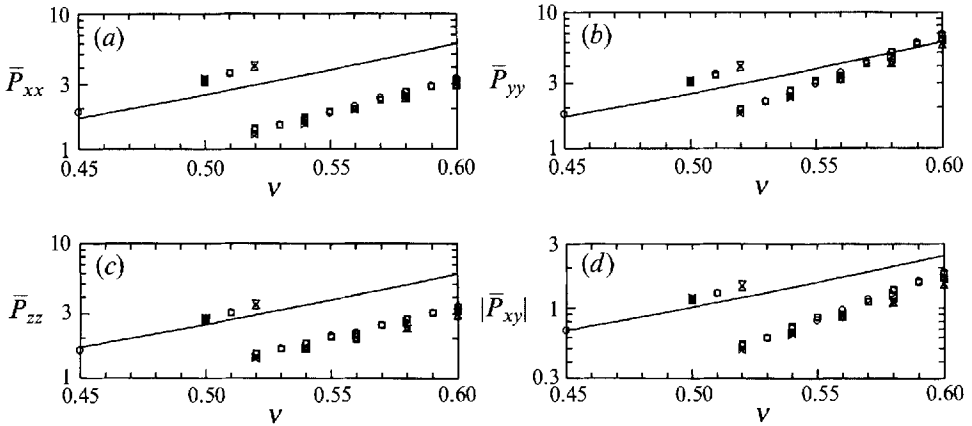


FIGURE 4. Non-dimensional (*a, b, c*) normal stresses and (*d*) shear stress versus solids fraction ν for simple shear flow. Comparison of present results for smooth spheres having $e = 0.8$ and initial control volumes in FCC arrays of $6 \times 6 \times 4$ (Δ , high T_{ti} ; ∇ , low T_{ti}), $4 \times 9 \times 4$ (\circ , high T_{ti} ; \square , low T_{ti}), and $4 \times 12 \times 4$ (\triangleright , high T_{ti} ; \triangleleft , low T_{ti}) with predictions of Lun (1991) (solid curves).

Richman (1989) and Walton, Kim & Rosato (1991) had investigated the phenomenon of stress anisotropy in the simple shear flow of smooth inelastic spheres by using kinetic theory and computer simulation respectively.

As shown in figures 2 and 3, the present results for stresses show first a decrease with increasing concentration to a minimum, and thereafter an increase with increasing concentration up to about 0.5. With further increase of ν , a couple of interesting phenomena occur. First, the present stresses suddenly decrease and then increase again with increasing ν . Secondly, at low concentrations \bar{P}_{zz} is somewhat larger than \bar{P}_{yy} , but for $\nu > 0.15$ the component \bar{P}_{zz} becomes small than \bar{P}_{yy} while \bar{P}_{xx} remains the largest one. At solids fractions higher than about 0.5, \bar{P}_{yy} becomes the largest component, and \bar{P}_{xx} falls a bit below \bar{P}_{zz} . Furthermore, the stresses obtained by Walton & Braun at $\nu = 0.6$ are higher than the present ones as shown in figure 3. Their \bar{P}_{yy} and \bar{P}_{xx} are nearly equal in magnitude whereas the present ones differ by a factor of almost two.

To help explain the peculiar behaviour of stresses at high concentrations found in the present simulations, some possible factors such as the dimensions of the control volume and the initial conditions were explored. More simulation results for stresses in simple shear flow of inelastic perfectly smooth spheres with $e = 0.8$ were obtained by using both high and low initial translational granular temperatures T_{ti} and control volumes with initial $6 \times 6 \times 4$, $4 \times 9 \times 4$ and $4 \times 12 \times 4$ FCC arrays as shown in figure 4. The abrupt changes in stresses for control volumes with initial $4 \times 9 \times 4$ and $4 \times 12 \times 4$ FCC arrays are found to occur at about $\nu = 0.52$, whereas those for a $6 \times 6 \times 4$ FCC array take place at about 0.53. Thereafter the stresses increase monotonically with increasing ν . Generally speaking, the stresses at $\nu > 0.52$ are found to depend only slightly upon the initial translational granular temperature T_{ti} and the dimensions of the control volume with initial FCC particle-array.

The flow field or control volume with an initial $4 \times 9 \times 4$ FCC array is evenly divided into nine layers. The ensemble average of particle number density for each layer is computed for observation. At $\nu = 0.52$ the height of the control volume H equals 8.267σ which means that each layer has a thickness of 0.918σ . At its turns out, for $\nu \geq 0.52$ no particle crosses the top and bottom boundaries of the control volume and

the particle number density for each layer remains unchanged. This indicates the ordering of particles in layers, with each particle caged by its nearest neighbours. As a result, the correlation of velocities among particles is enhanced. This is reflected in the results for the shear stress \bar{P}_{zy} . Although \bar{P}_{zy} is non-zero for most cases, its magnitude is often a couple of orders of magnitude smaller than the major shear stress \bar{P}_{xy} . For $\nu < 0.52$, \bar{P}_{zy} normally fluctuates with positive and negative values and changes from one layer to another. However, for $\nu \geq 0.52$, \bar{P}_{zy} becomes positive throughout the entire flow field even though its magnitude still remains relatively small. This shows that the particle velocities are correlated in the y - and z -directions in some fashion. Similar results are found for control volumes initially set up as $6 \times 6 \times 4$ and $4 \times 12 \times 4$ FCC arrays. The ordering of particles in layers, the formation of high-density microstructures and the increase in correlation of particle velocities are believed to be the major factors causing the abrupt changes and reordering of stress components at some critical concentrations.

In reality, there exists a natural geometric 'critical' point at $\nu = \pi/6$ or 0.5236; it represents the largest density in a simple cubic array in which layers of particles can move over one another unimpeded in the horizontal shearing plane. Above such a value, one might anticipate some kind of 'discontinuity' effect due to possible formation of microstructures of particles in the system. This is exactly what is observed in the present study. The macroscopic properties such as temperatures, particle spins and stresses at ν close to 0.52 exhibit 'jumps' in values. Note that systems with ν higher than 0.5236 are still shearable. This can be illustrated as follows. If we deform a small simple cubic array with $\nu = 0.5236$ into a parallelogram-based column by rotating two opposite sides 60° in the same direction, the solids fraction now becomes 0.6046. There can still be no resistance for particle layers moving over each other in the horizontal shearing plane since the column height remains an integer multiple of the particle diameter. The fact that the top and bottom periodic boundaries permit particles to travel back and forth brings about an additional degree of flexibility for shearing particles at solids fractions higher than 0.6046. As shown in figure 2, the highest solids fraction sheared in the present simulation is 0.65 for particles with $e = 0.95$.

Hoover & Ree (1968) obtained similar behaviour in pressures in their molecular dynamics study of thermo-equilibrium (i.e. no mean shear) phase transition of smooth elastic hard spheres and hard disks at high concentrations. In the case of hard spheres, the critical solids fraction was found to be between 0.46 and 0.48. They attributed the sudden decrease in pressure to the process of phase transition whereby the 'fluid phase' changed into a 'solid phase'. They investigated systems of 32, 108, 256 and 500 hard spheres and found that the dependence of properties on total particle number was not statistically significant.

Similar abrupt changes in mean pressure were reported by Walton & Braun (1986*b*) in their computer simulations for simple shear flow of two-dimensional inelastic, frictional disks with $e = 0.8$ and $\mu = 0.5$ at high solids area fraction > 0.775 . A solids area fraction of 0.7854 represents the largest density in a square packing at which strings of disks can overtake others unhindered in the streamwise direction. They used a 'soft-disk' collision model and the stresses were found to depend not only on particle concentrations but also on shear rates. Campbell & Brennen (1985) quantified the formation of microstructure in two-dimensional hard-disk Couette flows. Unfortunately, they studied systems with solids area fraction less than 0.775, and thus they did not observe any onset of stress jumps.

It is worth mentioning that there exist various types of instability in large simple shear systems of particles with low coefficient of restitution at low to moderate solids

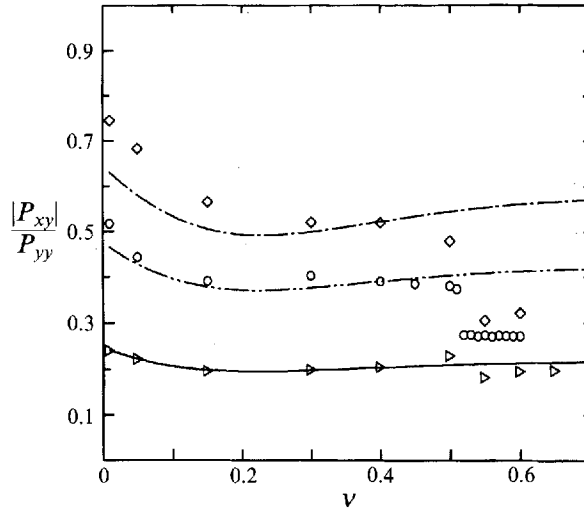


FIGURE 5. Stress ratio versus solids fraction for simple shear flow. Comparison of present results for smooth spheres (\diamond , $e = 0.6$; \circ , $e = 0.8$; \triangleright , $e = 0.95$) with predictions of Lun (1991) (— — —, $e = 0.6$; — — — — —, $e = 0.8$; — — — — —, $e = 0.95$).

concentrations. Hopkins, Jenkins & Louge (1992) found that for low values of restitution coefficient and low mean solids fraction, the mean velocity gradient was highly nonlinear and the granular temperature was much higher in the dilute regions than in the dense ones. In a study of linear stability of unbounded simple shear flow based on a kinetic theory, Savage (1992) found that the ‘instability’ increases with decreasing coefficient of restitution, and that simulations using relatively small control volumes are likely to be ‘stable’ whereas large control volumes with large numbers of particles are more likely to be ‘unstable’. Hopkins & Louge (1991) reported the formation of inelastic microstructures in simple shear flows of disks with low coefficient of restitutions at low solids concentrations. Babic (1992) performed a kinetic theory analysis for the linear stability of two-dimensional simple shear of disks and reached similar conclusions to those of Savage (1992). These instability mechanisms are believed to be different from the high-density ones that are responsible for the abrupt variations in properties at solids fraction near 0.52 as observed in the present study.

As mentioned earlier, the stresses at $\nu = 0.6$ obtained by Walton & Braun (1986*a*) for smooth sphere with $e = 0.8$ are higher than the present ones as shown in figure 3. Walton & Braun used a soft-sphere collision model. The particles were first randomly distributed in a control volume and then moved into positions such that particle overlaps were eliminated before the actual simulation began. It seems possible that the randomness of the initial particle positions at such high solids fraction of 0.6 and the fact that the stresses were shear-rate dependent could cause the stresses to be higher than the present results.

The variations of stress ratios for $e = 0.6$, 0.8 and 0.95 with solids fraction are plotted in figure 5. In general, there is good agreement between the present results and the predictions of Lun (1991). At ν near 0.52, the stress ratios clearly show abrupt reductions in values. For $\nu > 0.52$, the stress ratio becomes rather insensitive to the increase of solids fraction.

Figure 6 shows comparisons between the present results and those of Campbell (1989) for rough inelastic spheres with $e = 0.8$ and $\beta = 0$. Reasonable agreement between the two is found except at high solids fractions. By the way, the lowest solids

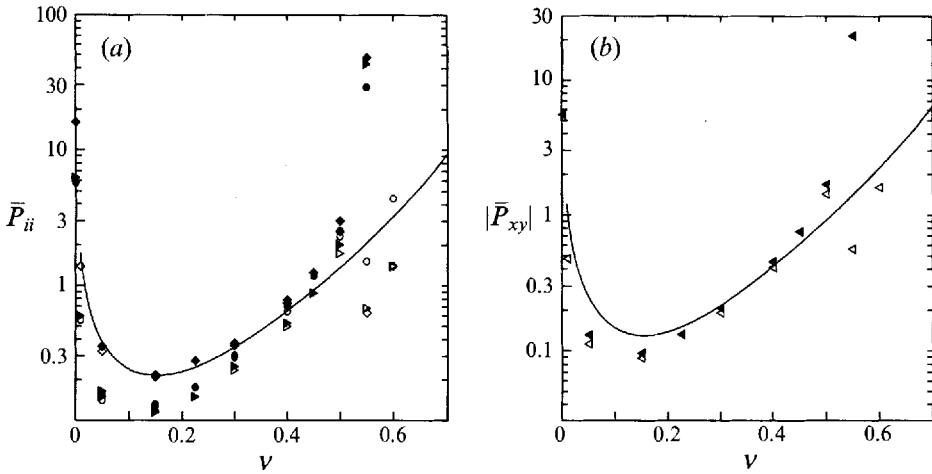


FIGURE 6. Non-dimensional (a) normal stresses and (b) shear stress versus solids fraction ν for simple shear flow. Comparison of present results for spheres having $e = 0.8$ and $\beta = 0$ (\diamond , \bar{P}_{xx} ; \circ , \bar{P}_{yy} ; \triangleright , \bar{P}_{zz} ; \triangleleft , $|\bar{P}_{xy}|$) with predictions of Lun (1991) (solid curve) and results of Campbell (1989) (\blacklozenge , \bar{P}_{xx} ; \bullet , \bar{P}_{yy} ; \blacktriangleright , \bar{P}_{zz} ; \blacktriangleleft , $|\bar{P}_{xy}|$).

fraction simulated by Campbell was $\nu = 0.001$ instead of 0.01 as printed in his paper (personal communication). At $\nu = 0.55$, Campbell's stresses are much higher than the present ones. The stress component \bar{P}_{xx} was found to be the largest one followed by \bar{P}_{zz} and then \bar{P}_{yy} , whereas the present results indicate that \bar{P}_{yy} is the largest component followed by \bar{P}_{zz} and \bar{P}_{xx} . Besides this, it is not clear why the stresses at $\nu = 0.55$ obtained by Campbell for spheres with $e = 0.8$ were in some cases higher than those for spheres with $e = 1.0$ (see figure 3 of Campbell's paper). Similar anomalies can also be observed for particles with $e = 0.4, 0.6$ and 0.8 at $\nu = 0.4, 0.45, 0.50$ and 0.55 in his paper. Such irregularities are not seen in the present simulations nor in the theoretical predictions of Lun (1991).

For realistic inelastic frictional particle collisions, the normal and tangential coefficients of restitution and the friction coefficient are *intricately* related. In order to study the effect of particle surface friction, we employ the information obtained from the experiments of Maw (1976) for steel spheres mentioned in §2. Inelastic particles with $e = 0.93$ and three different types of surface characteristics are simulated: namely, (i) perfectly smooth spheres with $\beta = -1$, (ii) frictional steel spheres with $\beta_0 = 0.4$ and $\mu = 0.123$, and (iii) spheres with infinite friction, i.e. $\beta = 0$. In figure 7, the simulation results for stresses are plotted together with the theoretical predictions of Lun (1991) and the experimental measurements obtained by Craig *et al.* (1986) in shearing carbon steel spheres at different solids concentrations and shear zone thickness, H , inside an annular shear cell.

Comparing the simulation results for perfectly smooth spheres with those of frictional spheres in figure 7, the stresses are found to decrease with increasing particle surface friction. The stresses for idealized particles with infinite friction are consistently lower than those for smooth spheres and frictional steel spheres. The reason is that a higher rate of energy dissipation is artificially incurred as the result of the elimination of post-collisional relative tangential velocities (or in other words the removal of part of the particle kinetic energy) in each binary collision of spheres with $\beta = 0$.

In their simulations of simple shear flow of two-dimensional disks with $e = 0.8$, Walton & Braun (1986*b*) found that at solids area fraction > 0.25 the stresses for

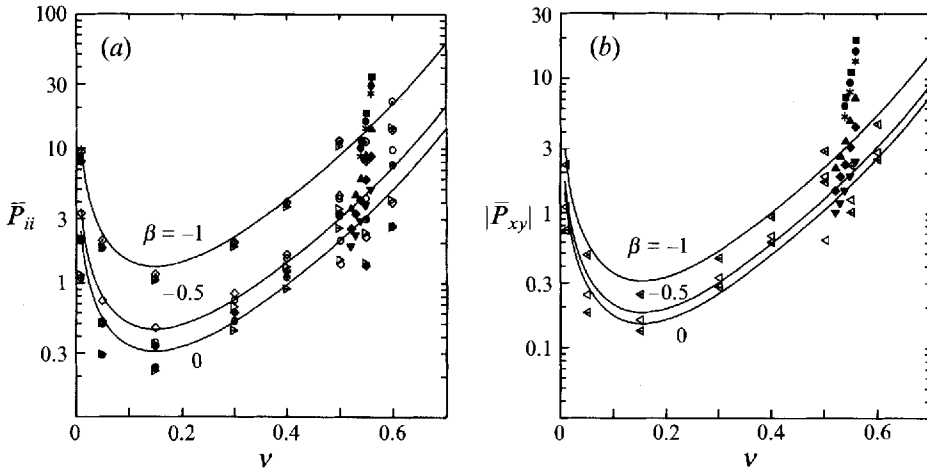


FIGURE 7. Non-dimensional (a) normal stresses and (b) shear stress versus solids fraction. Comparison of present results for spheres having $e = 0.93$ and (i) $\beta = -1$, (\diamond , \bar{P}_{xx} ; \odot , \bar{P}_{yy} ; \triangleright , \bar{P}_{zz} ; \triangleleft , $|\bar{P}_{xy}|$), (ii) $\beta_0 = 0.4$ and $\mu = 0.123$ (\diamond , \bar{P}_{xx} ; \circ , \bar{P}_{yy} ; \triangleright , \bar{P}_{zz} ; \triangleleft , $|\bar{P}_{xy}|$), and (iii) $\beta = 0$ (\oplus , \bar{P}_{xx} ; $\opl�$, \bar{P}_{yy} ; \triangleright , \bar{P}_{zz} ; \triangleleft , $|\bar{P}_{xy}|$) with predictions of Lun (1991) (solid curves) and test data of Craig *et al.* (1986) (\blacksquare , \bullet , $*$, \blacktriangle , \blacklozenge , \blacktriangledown for $H/\sigma = 12.9, 11.07, 9.23, 7.38, 5.54, 3.7$ and $\nu_{max} = 0.599, 0.601, 0.603, 0.612, 0.623, 0.652$ respectively).

shearing ‘soft disks’ with friction coefficient of $\mu = 0.5$ were consistently higher than those for perfectly smooth ones ($\mu = 0$). In other words, the stresses and granular temperatures were found to increase with increasing particle surface friction. This is contrary to the present simulation results and the predictions of the kinetic theories of Lun & Savage (1987) and Lun (1991) for hard spheres. Realistically, it is not obvious how the stresses and temperatures could increase in the case where supposedly higher rates of energy dissipation were incurred due to the presence of particle surface friction at the same shear rate. However, if the particles were *idealized* as perfectly or nearly perfectly rough, i.e. $\beta \rightarrow 1$, then as shown by Lun & Savage (1987) it would be possible for the stresses at concentrations where the collisional stresses are dominant to be higher than those for perfectly smooth spheres with identical e .

In general, the predictions of Lun (1991) compare favourably with the present simulation results, as shown in figures 6 and 7. The theory of Lun is expected to be best suited to systems of spheres with e close to unity and β close to -1 where the rate of energy dissipation is small. Fortunately, the theory yields reasonable predictions even for the case of $\beta = 0$ (figure 6). As mentioned previously, the coefficient of β in the kinetic theory of Lun represents a mean value averaged over the entire range of sticking and sliding contacts. Using $\beta = -0.5$, the theory seems to predict stresses that are compatible with the simulation results for frictional steel spheres with $\beta_0 = 0.4$ and $\mu = 0.123$ (figure 7).

Craig *et al.* (1986) carried out annular shear cell experiments using carbon steel spheres at high concentrations in the range of $0.521 \leq \nu \leq 0.559$. The mean values of the shear-layer thickness and the solids fractions at maximum closest packing for each H tested are given in the caption of figure 7. The stresses measured by Craig *et al.* were found to increase sharply with minor increase in solids fraction, and decrease with decreasing H , as shown in figure 7. Such variations of stresses could be caused by a number of factors such as finite-size effects of the sidewalls in the shearing zone, slip at the top and bottom solid boundaries, increase in correlations between particle

velocities, and the 'layering' effects of particles. Savage (1992) used numerical simulation to study the effects of shear-layer thickness on stresses developed in Couette flow of an assembly of idealized smooth spheres and found similar reductions in stresses with decreasing H at solids concentrations even much lower than those in experiments. Further study in this area is required for inelastic frictional spheres. In passing, it is necessary to point out that Craig *et al.* did not determine the coefficient of restitution and friction coefficient for the carbon-steel spheres tested. The material properties of the carbon-steel spheres could differ from those of the steel ball bearings used by Maw (1976) and the present simulations.

Abrupt changes in stresses similar to those observed previously in figure 3 for smooth spheres with $e = 0.8$ at $\nu \approx 0.52$ are also found in the present simulation results for the three types of particles with $e = 0.93$, as shown in figure 7. The dimensions of the control volume and the initial translational granular temperature are varied, as was done previously for the case of frictional steel spheres with $e = 0.93$, $\beta_0 = 0.4$ and $\mu = 0.123$. The critical solids fraction is found to occur first at about 0.50 instead of 0.52 as in the previous case. The difference in critical ν is probably caused by the additional degrees of freedom of interactions between particles through rotational motion as a result of surface friction. Other than that, the stresses are found to behave qualitatively similarly to those shown in figure 4 for smooth spheres with $e = 0.8$; thus they are not presented here.

There is evidence for stress reductions at some critical high solids fractions in some experiments of Savage & Sayed (1984); for example, in tests of polystyrene beads (PSI, 1.1 mm mean diameter) and glass beads (1.8 mm mean diameter) at $\nu = 0.50$. The phenomenon is best seen in figures 2 and 4 of Lun (1991). Lun plotted the experimental results for stresses using only those data that were recorded at the highest shear rates for each solids fraction of material tested. This minimized the influence of quasi-static effects which can occur at low shearing rates of bulk materials.

No abrupt changes in stresses were found in the data of Craig *et al.* (1986). The reason is that the range of $0.521 \leq \nu \leq 0.559$ tested in the experiments was beyond the critical solids fraction of 0.50. For a similar reason, the stresses presented by Hanes & Inman (1985) in shearing glass beads of 1.85 mm mean diameter show no abrupt variations because the largest solids fraction tested was 0.49. Hanes & Inman also tested 1.1 mm mean diameter glass beads in the range of $0.37 \leq \nu \leq 0.56$; however the stresses behaved rather differently from all other theoretical, numerical and experimental results.

In conjunction with stress results shown in figure 7, the stress ratio $|P_{xy}|/P_{yy}$ for inelastic frictional spheres is plotted versus solids fraction in figure 8. In general, there is good agreement between the predictions of Lun (1991) and the present results. The variations of stress ratios for frictional spheres (figure 8) with solids fraction are similar to those for smooth spheres (figure 5).

Some interesting auxiliary information that can be obtained from the simulations concerns for example angular momentum flux \mathbf{L} , ratio of rotational temperature T_r to translational temperature T_t , mean particle spin ω_0 , ratio of the number of sticking contacts to the total number of collisions N_s , and mean free path λ .

The angular momentum flux \mathbf{L} , sometimes called the couple stresses, is composed of the sum of a kinetic part and a collisional transfer part. The results for shearing frictional steel spheres with $e = 0.93$, $\beta_0 = 0.4$ and $\mu = 0.123$ at different concentrations show that the couple stresses are in general at least a couple of orders of magnitude smaller than the normal and shear stresses and for all practical purposes they may be neglected. This finding supports the results obtained earlier by Lun (1991) that the

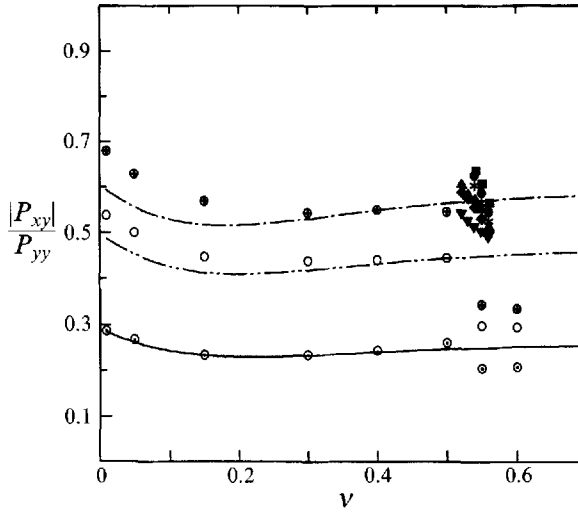


FIGURE 8. Stress ratio versus solids fraction. Comparison of present results for spheres having $e = 0.93$ (\odot , $\beta = -1$; \circ , $\beta_0 = 0.4$ and $\mu = 0.123$; \oplus , $\beta = 0$) with predictions of Lun (1991) (—, $\beta = -1$; - - - - - , $\beta = -0.5$; - · - · - · , $\beta = 0$) and data of Craig *et al.* (1986; symbols are same as those in figure 7 caption).

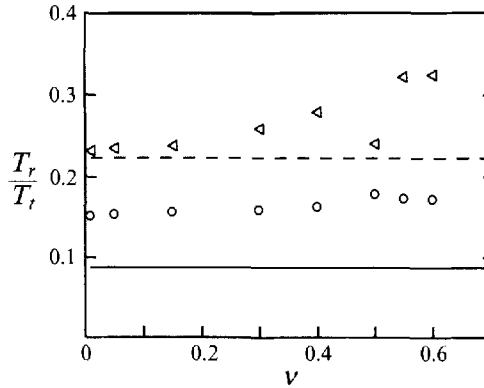


FIGURE 9. Variation of granular temperature ratio with solids fraction ν for the case of simple shear. Comparison of present results for frictional spheres having $e = 0.93$ (\circ , $\beta_0 = 0.4$ and $\mu = 0.123$; \triangleleft , $\beta = 0$) with predictions of Lun (1991) (—, $\beta = -0.5$; - - - , $\beta = 0$).

couple stress tensor is identically zero in the kinetic theory of the first-order gradient of macroscopic flow variables for systems of slightly inelastic, slightly rough spheres. In a polar fluid, the couple stresses are functions of gradients of particle spin. In the present case of simple shear flow, where the particle spin is practically uniform across the flow field, it is not surprising to see that the couple stresses are essentially zero.

According to the kinetic theory of Lun the ratio of rotational temperature to translational temperature, T_r/T_t , is a function of tangential coefficient of restitution only and independent of solids concentration. In figure 9, the simulation results for T_r/T_t in the simple shear flow of steel spheres with $e = 0.93$, $\beta_0 = 0.4$ and $\mu = 0.123$ exhibit only slight variation with ν while those for spheres with $e = 0.93$ and $\beta = 0$ show a relatively more pronounced dependence on ν . In the case of $\beta = 0$, both the present results and the theoretical predictions of Lun show reasonable agreement.

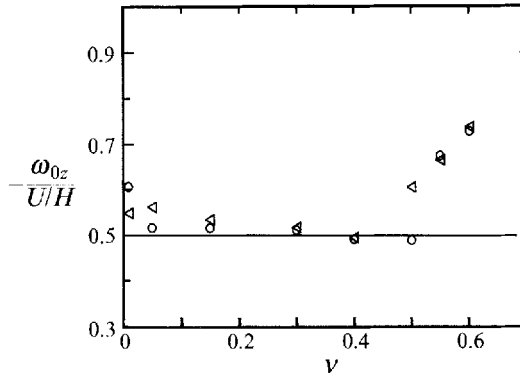


FIGURE 10. Variation of non-dimensional mean spin with solids fraction ν for the case of simple shear. Comparison of present results for frictional spheres having $e = 0.93$ (\circ , $\beta_0 = 0.4$ and $\mu = 0.123$; \triangle , $\beta = 0$) with prediction of Lun (1991) (solid curve).

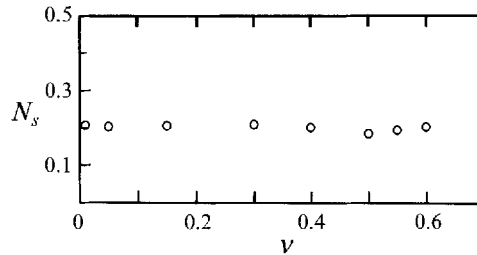


FIGURE 11. Ratio of number of sticking contacts to total number of collisions per particle N_s versus solids fraction for spheres with $e = 0.93$, $\beta_0 = 0.4$ and $\mu = 0.123$.

Since a constant $\beta = -0.5$ was used in the kinetic theory of Lun, the theoretical predictions for T_r/T_t are somewhat different to the present simulation results obtained by using a more realistic collision model.

Figure 10 shows the variation of the non-dimensional mean particle spin with solids fraction. The theory of Lun (1991) predicts that the mean spin for simple shear flow is one half of the vorticity, i.e. $\omega_0 = -\frac{1}{2}\nabla \times \mathbf{u}$. In terms of the present coordinate system, the non-dimensional mean spin can be written as $-\omega_{0z}/(du/dy) = 0.5$. As shown in figure 10, the theoretical predictions compare favourably with the present simulation results except at extreme values of ν where the anisotropy in temperature distributions and the particle layering effects play important roles.

It is interesting to see that the ratio of the number of sticking contacts to the total number of collisions per particle N_s (for the simple shear flow of inelastic frictional spheres with $e = 0.93$, $\beta_0 = 0.4$ and $\nu = 0.123$) is independent of the solids concentration, as shown in figure 11, whereas intuition may say otherwise. The number of sticking contacts constitutes approximately 20% of the total number of collisions per particle while the other 80% are sliding contacts. Note that N_s represents a ratio averaged over all possible orientations of particle collisions. Although the distribution of contact angles changes with solids fraction, the ratio can possibly remain unaffected.

The mean free path λ represents the mean free flight distance traversed by a particle between successive collisions and it may be defined as the ratio of the total distance travelled by a particle to the total number of its collisions within a certain period of time. As shown in figure 12 the variations of λ for perfectly smooth spheres with

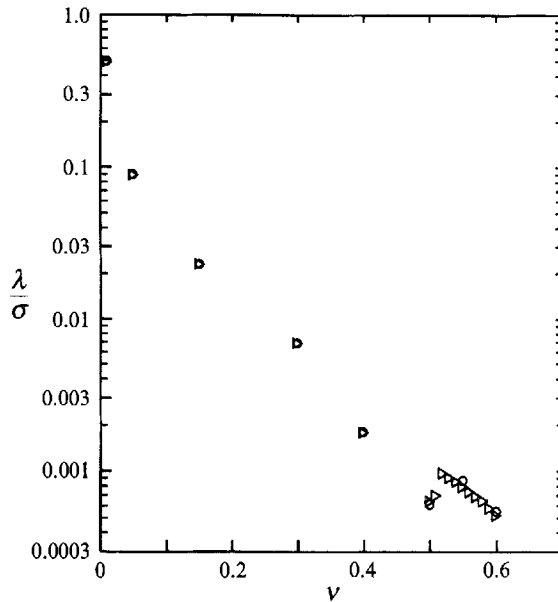


FIGURE 12. Variation of non-dimensional mean free path with solids fraction ν for the case of simple shear flow; \triangleright , perfectly smooth spheres with $e = 0.8$; \circ , frictional steel spheres with $e = 0.93$, $\beta_0 = 0.4$ and $\mu = 0.123$.

$e = 0.8$ are almost identical to those for spheres with $e = 0.93$, $\beta_0 = 0.4$ and $\mu = 0.123$. This signifies that the mean free path is basically independent of material properties such as the coefficient of restitution and the friction coefficient. This is not surprising because the bulk material is simply composed of idealized hard spheres with no potential forces such as electrostatic forces; thus the mean free path is mainly a function of solids concentration.

5. Conclusion

The present research utilizes the approach of molecular-dynamics-type computer simulations for the simple shear flow of granular material inside a control volume. Real collisions of inelastic frictional spheres are imitated by a simple sticking–sliding hard-sphere collision model. Such an instantaneous hard-sphere binary collision model breaks down at high bulk concentrations where simultaneous multiple-particle contacts are frequent. Nevertheless, valuable information about flow properties can still be gained by this approach for low to moderately high solids fractions.

After the flow has reach a steady state, macroscopic flow properties such as stresses, granular temperatures and mean free path are obtained by means of ensemble averages. The stresses are found to be anisotropic and decrease with decreasing coefficient of restitution and increasing friction coefficient. Variations in initial conditions such as using high and low granular temperatures and different sizes of control volume based on initial FCC arrays have no significant effects on the results. Generally speaking, the present simulation is in favourable agreement with previous theoretical, numerical and experimental investigations. At high solids fraction, above about 0.50, a critical concentration is found to exist where the majority of the flow properties such as stresses and mean particle spin experience abrupt changes. The critical solids fraction for simple shear flows of smooth inelastic spheres occurs at about 0.52 whereas that for

frictional inelastic spheres occurs at about 0.50. The layering effects of particles, the formation of high-density microstructures and the increase in correlation of particle velocities are major factors in causing the sudden variations.

Future studies using computer simulations with different initial regular particle packing procedures and random distributions at high solids fractions will be beneficial for a better understanding of the flow behaviour at high solids concentrations.

Grateful acknowledgement is made to the Natural Sciences and Engineering Research Council of Canada (NSERC) for support of this work through an NSERC operating grant. Mr A. A. Bent was partially supported by an NSERC University Undergraduate Student Research Award. The authors are indebted to Dr N. Maw for the permission to obtain a copy of his original data.

REFERENCES

- ALLEN, M. P. & TILDESLEY, D. J. 1987 *Computer Simulation of Liquids*. Oxford University Press.
- BABIC, M. 1992 Particle clustering: an instability of rapid granular flows. In *Advances in Micromechanics of Granular Materials* (ed. H. Shen, M. Satake, M. Mehrabadi, C. S. Chang & C. S. Campbell). Elsevier.
- CAMPBELL, C. S. 1986 Computer simulation of rapid granular flows. *Proc. US Natl Congr. Appl. Mech., 10th Austin, TX*, pp. 327–338.
- CAMPBELL, C. S. 1989 The stress tensor for simple shear flows of a granular material. *J. Fluid Mech.* **203**, 449–473.
- CAMPBELL, C. S. 1990 Rapid granular flows. *Ann. Rev. Fluid Mech* **22**, 57–92.
- CAMPBELL, C. S. & BRENNEN, C. E. 1985 Computer simulation of granular shear flows. *J. Fluid Mech.* **151**, 167–188.
- CARNAHAN, N. F. & STARLING, K. E. 1969 Equations of state for non-attracting rigid spheres. *J. Chem. Phys.* **51**, 635–636.
- CRAIG, K., BUCKHOLZ, R. H. & DOMOTO, G. 1986 An experimental study of the rapid flow of dry cohesionless metal powders. *Trans. ASME E: J. Appl. Mech.* **53**, 935–942.
- CRAIG, K., BUCKHOLZ, R. H. & DOMOTO, G. 1987 Effects of shear surface boundaries on stress for shearing flow of dry metal powders – an experimental study. *Trans. ASME K: J. Tribol.* **109**, 232–237.
- GOLDSMITH, W. 1960 *Impact: The Theory and Physical Behavior of Colliding Solids*. E. Arnold.
- HANES, D. M. & INMAN, D. L. 1985 Observations of rapidly flowing granular-fluid materials. *J. Fluid Mech.* **150**, 357–380.
- HOOVER, W. G. & REE, F. H. 1968 Melting transition and communal entropy for hard spheres. *J. Chem. Phys.* **49**, 3609–3617.
- HOPKINS, M. A., JENKINS, J. T. & LOUGE, M. Y. 1992 On the structure of 3D shear flows. In *Advances in Micromechanics of Granular Materials* (ed. H. Shen, M. Satake, M. Mehrabadi, C. S. Chang & C. S. Campbell). Elsevier.
- HOPKINS, M. A. & LOUGE, M. Y. 1991 Inelastic microstructure in rapid granular flows of smooth disks. *Phys. Fluids A* **3**, 47–57.
- JENKINS, J. T. 1987 Rapid flows of granular materials. In *Non-classical Continuum Mechanics: Abstract Techniques and Applications* (ed. R. J. Knops & A. A. Lacey). Cambridge University Press.
- JENKINS, J. T. & RICHMAN, M. W. 1985 Grad's 13-moment system for a dense gas of inelastic spheres. *Arch. Rat. Mech. Anal.* **87**, 355–377.
- JOHNSON, K. L. 1982 One hundred years of Hertz contact. *Proc. Inst. Mech. Engrs* **196**, 363–378.
- LEES, A. W. & EDWARDS, S. F. 1972 The computer study of transport processes under extreme conditions. *J. Phys. C: Solid State Phys.* **5**, 1921–1929.
- LUN, C. K. K. 1991 Kinetic theory for granular flow of dense, slightly inelastic, slightly rough spheres. *J. Fluid Mech.* **233**, 539–559.

- LUN, C. K. K. & SAVAGE, S. B. 1987 A simple kinetic theory for granular flow of rough, inelastic, spherical particles. *Trans. ASME E: J. Appl. Mech.* **54**, 47–53.
- LUN, C. K. K., SAVAGE, S. B., JEFFREY, D. J. & CHEPURNIY, N. 1984 Kinetic theories for granular flow: inelastic particles in Couette flow and slightly inelastic particles in a general flowfield. *J. Fluid Mech.* **140**, 223–256.
- MAW, N. 1976 A theoretical and experimental investigation into the impact and rebound of elastic bodies. PhD thesis, CNAAP, Sunderland Polytechnic, UK.
- MAW, N., BARBER, J. R. & FAWCETT, J. N. 1976 The oblique impact of elastic spheres. *Wear* **38**, 101–114.
- MAW, N., BARBER, J. R. & FAWCETT, J. N. 1981 The role of elastic tangential compliance in oblique impact. *Trans ASME F: J. Lubrication Technol.* **103**, 74–80.
- NAKAGAWA, M. 1988 Kinetic theoretical approach for rapidly deforming granular material. In *Micromechanics of Granular Materials* (ed. M. Sataka & J. T. Jenkins). Elsevier.
- RICHMAN, M. W. 1986 Kinetic theories for rate dependent granular flows. *Proc. US Natl Congr. Appl. Mech, 10th Austin, TX* pp. 339–366.
- RICHMAN, M. W. 1989 The source of 2nd moment in dilute granular flows of highly inelastic spheres. *J. Rheol.* **33**, 1293–1306.
- SAVAGE, S. B. 1989 Flow of granular materials. In *Theoretical and Applied Mechanics* (ed. P. Germain, M. Piau & D. Caillerie). Elsevier.
- SAVAGE, S. B. 1992 Numerical simulations of Couette flow of granular materials; spatio-temporal coherence and $1/f$ noise. In *Physics of Granular Media* (ed. J. Dodds & D. Bideau), pp. 343–362. New York: Nova Science.
- SAVAGE, S. B. 1993 Disorder, diffusion and structure formation in granular flows. In *Disorder and Granular Media* (ed. D. Bideau). North-Holland.
- SAVAGE, S. B. & SAYED, M. 1984 Stresses developed by dry cohesionless granular materials sheared in an annular shear cell. *J. Fluid Mech.* **142**, 391–430.
- WALTON, O. R. 1988 Granular solids flow project quarterly report. *Rep UCID-20297-88-1*. Lawrence Livermore Lab., University of California.
- WALTON, O. R. & BRAUN, R. L. 1986a Stress calculations for assemblies for inelastic spheres in uniform shear. *Acta Mech.* **63**, 73–86.
- WALTON, O. R. & BRAUN, R. L. 1986b Viscosity and temperature calculations for shearing assemblies of inelastic, frictional disks. *J. Rheol.* **30**, 949–980.
- WALTON, O. R., KIM, H. & ROSATO, A. D. 1991 Micro-structure and stress difference in shearing flows of granular materials. *Proc. ASCE Engng Mech. Div. Conf., Columbus, Ohio, May 19–21, 1991*.